

# Controlled Burning of Forest Detritus Altering Spectroscopic Characteristics and Chlorine Reactivity of Dissolved Organic Matter: Effects of Temperature and Oxygen Availability

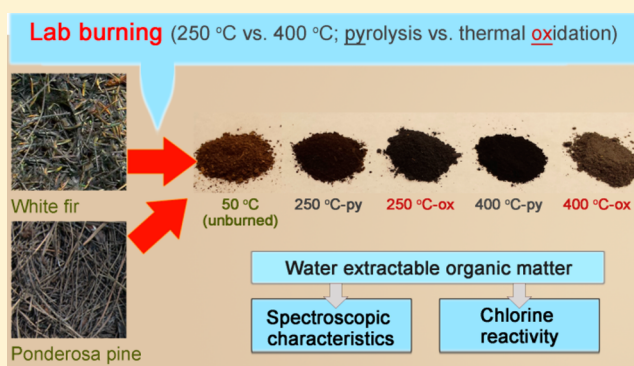
Jun-Jian Wang,<sup>†</sup> Randy A. Dahlgren,<sup>‡</sup> and Alex T. Chow<sup>\*,†</sup>

<sup>†</sup>Baruch Institute of Coastal Ecology & Forest Science, Clemson University, Georgetown, South Carolina 29442, United States

<sup>‡</sup>Department of Land, Air and Water Resources, University of California, Davis, California 95616, United States;

## S Supporting Information

**ABSTRACT:** Forest fires occur with increasing frequency and severity in the western United States, potentially altering the chemistry and quantity of dissolved organic matter (DOM) and disinfection byproduct (DBP) precursors exported from forested watersheds. However, little is known concerning effects of the fire triangle (heat, oxygen, and fuel) on DOM alteration. Using detritus from *Pinus ponderosa* and *Abies concolor* (dominant species in forests in the western United States), we prepared DOM from unburned and burned detritus under hypoxic (pyrolysis) and oxic conditions (thermal oxidation) at 250 and 400 °C. DOM characteristics and chlorine reactivity were evaluated by absorption and fluorescence spectroscopy and chlorination-based DBP formation potential tests. Spectroscopic results suggest that burned-detritus extracts had lower molecular weight (reflected by increased E2:E3 and fluorescence index) and divergent aromaticity (reflected by SUVA<sub>254</sub>) depending on oxygen availability. Temperature and oxygen availability interacted to alter the chlorine reactivity of fire-affected DOM. Increasing temperature from 50 to 400 °C resulted in decreased reactivities for trihalomethane and chloral hydrate formation and divergent reactivities for haloacetonitrile formation (unchanged for pyrolysis and increased for oxidation) and haloketone formation (increased for pyrolysis and decreased for oxidation). We demonstrate that DBP precursors in fire-affected forest detritus are highly dependent on temperature and oxygen availability.



## INTRODUCTION

Globally, forest watersheds are critical sources of water supply for billions of people,<sup>1</sup> with an estimated economic value for water storage and filtration of \$4.1 trillion per year.<sup>2</sup> Driven by climate change and increasing human presence in forests, wildfire frequency and intensity have been remarkably increased in recent decades, particularly in western North America.<sup>3,4</sup> As consequences of forest fires, deterioration of downstream water quality, including increased loads of sediments, nutrients, metals, and polycyclic aromatic hydrocarbons, may lead to potential threats to aquatic ecosystems and increased cost of clean water supply.<sup>1,5–7</sup> Forest wildfire can also alter the bulk organic matter chemistry of forest detritus by thermal reactions (such as oxygen-limited pyrolysis and thermal oxidation with oxygen)<sup>8,9</sup> and, thus, affect the load and chemistry of dissolved organic matter (DOM) to waterbodies.<sup>10,11</sup>

Safe drinking water is an important demand for public health,<sup>12,13</sup> but drinking water quality (e.g., DOM and disinfection byproducts (DBPs)) is very sensitive to landscape/ecosystem changes as affected by changing climate and natural/anthropogenic disturbances.<sup>14,15</sup> Recent case studies revealed that forest fires alter DOM chemistry and thus DBP

formation in drinking water, such as the possibly carcinogenic trihalomethanes (THMs), haloacetic acids (HAAs), and haloacetonitriles (HANs).<sup>16–18</sup> With greater wildfire severity, wildfires can potentially decrease the reactivity of terrestrial DOM in forming carbonaceous DBPs such as USEPA-regulated THMs and HAAs but increase the reactivity for forming more carcinogenic nitrogenous DBPs such as HANs and N-nitrosodimethylamine and brominated DBPs such as dichlorobromomethane.<sup>16</sup> As the nitrogenous DBPs have been found to be much more toxic and carcinogenic than the commonly regulated carbonaceous DBPs,<sup>19</sup> Wang et al.<sup>16</sup> proposed that particular attention should be placed on the nitrogenous DBP precursors in fire-affected watersheds. However, it is still not clear how the elements of the fire triangle (i.e., heat, oxygen, and fuel) interact to alter terrestrial DOM chemistry, which is critically important information for future modeling and assessment of fire effects on water quality and future water

Received: August 14, 2015

Revised: October 20, 2015

Accepted: October 23, 2015

Published: October 23, 2015

supply. As multiple interacting environmental factors lead to a large uncertainty in interpreting field fire effects, laboratory-controlled burn experiments can more effectively assess the effects of single or multiple factors on alteration of DOM and DBP formation resulting from fire.

Using a controlled-lab-burning approach, the thermogenic products (e.g., biochar, charcoal, black carbon, or ash) from various biomass (feedstock) sources have been characterized and demonstrate a high dependence on biomass source, temperature, oxygen, and reaction time.<sup>20–23</sup> In contrast, there is limited knowledge concerning the effects of variable fire conditions on DOM chemistry and chlorine reactivity.<sup>24–26</sup> Recently, Lin et al.<sup>27</sup> used liquid chromatography and organic carbon detection to characterize DOM from hotwater extracts of sawdust biochar and found increasing pyrolysis temperature (450 to 550 °C) resulted in a decrease of DOM, an increase of low molecular weight acids (from 3 to 42%), and a decrease of humic substances (from 16 to 4%). Uchimiya et al.<sup>24</sup> used excitation–emission matrix (EEM) fluorescence spectroscopy and PARAFAC analysis to characterize the DOM of biochar from distinct feedstock sources and pyrolysis temperatures and found a dependence of DOM chemistry on feedstock source, an increase of (poly)phenolic pyrolysis products and other water-soluble aromatic structures, and a decrease of humic-like structures with increasing temperature. Despite such progress in understanding DOM chemistry from charred materials, it remains poorly understood how DOM chemistry of forest detritus changes under hypoxic (defined as “pyrolysis” in this study) and oxic (defined as “thermal oxidation” in this study) conditions associated with wildfires. In addition, there is no knowledge concerning how chlorine reactivity and DBP formation of DOM is altered by contrasting wildfire conditions (temperature and oxygen availability).

To fill this knowledge gap, we focused on the effects of temperature (250 and 400 °C) and oxygen availability (pyrolysis and thermal oxidation) on DOM chemistry and its chlorine reactivity in water extracts of forest detritus from ponderosa pine (*Pinus ponderosa*) and white fir (*Abies concolor*) detritus collected outside the 2013 Rim Fire perimeter in Stanislaus National Forest (California). The temperature selection was based on the common range of historical fire temperatures<sup>28</sup> for the soil surface to represent low (250 °C) and high (400 °C) fire intensity conditions in coniferous forests. The results of this study are compared with a previous field study within the Rim Fire to better understand the specific effects of each fire element (heat, oxygen, and fuel source) on DOM chemistry and reactivity in DBP formation.

## MATERIALS AND METHODS

**Sample Source and Ash Preparation.** In January 2014, ~10 kg of nonburned detritus was collected from the surface of soils (0–5 cm) beneath ponderosa pine and white fir in the Stanislaus National Forest of California outside of the 2013 Rim Fire perimeter (Figure S1), as described in a previous study.<sup>16</sup> The detritus collection site has a mean annual precipitation of ~920 mm and mean annual temperature of ~15 °C (7 °C for January and 24 °C for July). The detritus materials were air-dried and well mixed using a clean metal bucket. Detritus materials were not ground before burning to better simulate field burning conditions. Approximately 30.0 g of dried detritus (containing ~30% foliar litter, ~10% twigs, ~10% bark, and ~50% unrecognizable duff) was placed on two-layers of heavy duty aluminum foil (10 × 30 cm), either

wrapped or unwrapped (defined as “pyrolysis” and “thermal oxidation”, respectively), and placed in a preheated muffle furnace at 250 or 400 °C for 1 h. The operational definition of “pyrolysis” in this study implies virtual absence of oxygen as only a trace amount of air (<15 mL) was present in the closed wrapped system, creating an oxygen-restricting environment to pyrolyze the sample. We calculate that >50 L of air would be required to completely oxidize the 30 g detritus sample. Therefore, we believe the laboratory burning is similar to field conditions forming ash or charcoal in which the pyrogenic organic matter or pyrogenic carbon is not generated from an absolutely oxygen-free environment but more likely an oxygen-restricting environment.<sup>29</sup> After 1 h of burning, samples were removed from the furnace and cooled to room temperature. Each heating treatment was replicated twice. The samples were identified by the heating temperature and heating type, for example, 250py and 250ox represent samples pyrolyzed and thermally oxidized at 250 °C, respectively. A total of five treatments were analyzed for each tree species: unburned (50 °C dried), 250py, 250ox, 400py, and 400ox. All sample weights were recorded before and after heating to determine mass loss. As presented in Figure S2, the pyrogenic detritus consistently showed black color, while the detritus burned at 400 °C showed gray color, which is consistent with previous interpretations of ash color in wildfire studies.<sup>28</sup>

**Extraction of Dissolved Organic Matter.** DOM was extracted from ash materials and ground unburned detritus (sieved through 1 mm screen). A 4.00 g sample was mixed with 200 mL Milli-Q water in a 250 mL Erlenmeyer flask at room temperature for 2 h at a rotary speed of 250 rpm.<sup>16</sup> After filtration using a prerinsed 0.45 µm poly(ether sulfone) membrane filter, filtrates were measured for dissolved organic carbon (DOC) and total dissolved nitrogen (TDN) using a Shimadzu TOC/TN analyzer, and ammonia/ammonium-N ( $\text{NH}_4^+\text{-N}$ ) and nitrate/nitrite-N ( $\text{NO}_x^-\text{-N}$ ) using a Sysmex Easychem discrete analyzer as described in a previous study.<sup>30</sup> The postburn DOC and TDN yields from the original detritus (mg/g-original-detritus) were calculated as the extractability of burned litter (mg/g-burned-detritus) multiplied by the percent mass remaining of burned material compared to original material (g-burned-detritus/g-original-detritus).

The UV–vis absorption and fluorescence excitation–emission matrix (EEM) of the DOM was determined respectively by a Shimadzu UV-1800 spectrophotometer (scan range, 200–700 nm) and Shimadzu spectrofluorometer RF5301 [emission (Em), 200–550 nm with 1 nm interval; excitation (Ex), 220–450 nm with 5 nm interval; slit width, 5 nm].<sup>31</sup> Specific UV absorbance at 254 nm ( $\text{SUVA}_{254}$ ; in  $\text{L mg C}^{-1} \text{ m}^{-1}$ ), a widely used indicator for DOM aromaticity, was calculated by dividing the UV absorbance at 254 nm by DOC concentration.<sup>32</sup> The E2/E3 ratio, an indicator of molecular weight of DOM, was calculated by dividing the absorbance at 254 nm by that at 365 nm.<sup>33</sup> The raw EEM was corrected following the method in Murphy et al.<sup>34</sup> After correction, fluorescence regional integration based on Simpson’s rule (FRI-SR) was used to divide the EEM into five operationally defined regions to characterize the DOM composition: I-tyrosine-like; II-tryptophan-like; III-fulvic acid-like; IV-soluble microbial byproduct-like; and V-humic acid-like.<sup>31,35</sup> The percent fluorescence response in each region ( $P_{i,n}$ ) was calculated as the proportion of area-normalized volume in region *i* to the entire region.

In the fluorescence EEM, the M peak around Ex < 250 and 290–325 nm, Em 370–430 nm indicates “marine-humic-like” component that is characteristic of aquatic sources.<sup>36</sup> The A peak around Ex < 260 nm, Em 448–480 nm and C peak around Ex < 250 nm and 320–360 nm, Em 420–460 nm indicate “terrestrial-humic-like” components that are mainly derived from terrestrial plant/soil organic matter.<sup>36</sup> The fluorescence index (FI), a common index to differentiate the microbial or terrestrial origin of DOM (~1.8 for microbial origin and ~1.2 for terrestrial origin), was determined as the ratio of fluorescence responses at Em 470 and Em 520 nm, at Ex 370 nm.<sup>37</sup> The freshness index ( $\beta/\alpha$ ), an index for the relative abundance of recently produced autochthonous DOM, was calculated as the fluorescence response at Em 380 nm divided by the maximum response between Em 420 and 435 nm, at Ex 310 nm.<sup>38</sup> The humification index (HIX), an index for the relative abundance of humic substances, was calculated as the area under the emission spectra at 435–480 nm divided by the peak area at 300–345 nm, at Ex 254 nm.<sup>39</sup> Finally, to explore whether the redox status of DOM was altered by different burning treatments, the Cory and McKnight PARAFAC model was used to calculate the redox index (RI) based on the corrected EEM.<sup>37</sup>

**Disinfection Byproduct Formation.** The chlorine reactivity of the DOM in forming DBP species was evaluated using the disinfection formation potential (FP) test.<sup>16,40,41</sup> All water extracts were diluted to a DOC concentration of  $\leq 3$  mg/L, buffered to pH 8.0 ( $\text{H}_3\text{BO}_3/\text{NaOH}$ ), and chlorinated with freshly prepared  $\text{NaOCl}/\text{H}_3\text{BO}_3$  solution (pH 8.0) at 25 °C in a 65 mL glass vial in the dark for 24 h without headspace. The chlorine dose was based on the organic and inorganic chlorine demand calculated from  $[\text{Cl}_2] = (3 \times [\text{DOC}]) + (7.6 \times [\text{NH}_3])$  based on mass concentration.<sup>40</sup> After quenching of the residual chlorine by 10%  $\text{Na}_2\text{SO}_3$  solution, DBPs were liquid–liquid extracted with MTBE and quantified by GC-ECD (Agilent 7890) strictly following EPA method 551.1.<sup>42</sup> This study quantified four THMs (trichloro-, dichlorobromo-, dibromochloro-, and tribromo-methanes), four HANs (trichloro-, dichloro-, bromochloro-, and dibromo-acetonitriles), three HKs (1,1-dichloro-2-, 1,1,1-trichloro-2-, 1,2,3-trichloropropanones), and CHD. All glassware and pipet tips were prechlorinated, acid-washed, Milli-Q-water-washed, and oven-dried (450 °C and 4 h for glassware and 50 °C for pipet tips) to remove potential contaminants. The minimum reporting levels (MRLs) for all DBP species were approximately 0.1–0.3  $\mu\text{g}/\text{L}$ .

The DOM reactivity in forming DBPs was expressed as specific DBP-FP (SDBP-FP;  $\mu\text{g}\text{-DBP}/\text{mg}\text{-DOC}$ ), which was calculated as the DBP concentration divided by the initial DOC concentration. The estimated DBP formation potential from source materials, or DBP-FP (in  $\mu\text{g}\text{-DBP}/\text{g}\text{-detritus}$ ), was calculated as the SDBP-FP in  $\mu\text{g}\text{-DBP}/\text{mg}\text{-DOC}$  multiplied by the DOC content of the source material ( $\text{mg}\text{-DOC}/\text{g}\text{-original-detritus}$ ). To evaluate the abundance of brominated DBPs, the bromine incorporation factor (BIF) for THMs and HANs was calculated as the total moles of Br atoms divided by the total moles of Cl plus Br atoms in the four THMs and the three dihaloacetonitriles.<sup>43</sup>

**Statistical Analyses.** Differences between characterization parameters (e.g., DOC, TDN, optical indices of extract, SDBP-FP, and DBP-FP) of unburned versus burned samples were evaluated using independent *t*-tests. The effects of temperature (250 versus 400 °C), oxygen availability (pyrolysis vs oxidation), vegetation type (pine vs fir) and their interactions

in influencing the SDBP-FP of detritus extracts and DBP-FP in burned detritus were assessed using a three-way ANOVA. Pearson's correlations among the spectroscopic characteristics and the chlorine reactivity (SDBP-FP) of DOM were conducted, and a principal component analysis was conducted to reduce the dimensions of different DOM parameter as all the prerequisites (such as normality tests, KMO measurement, and Bartlett's tests) were satisfied.

## RESULTS AND DISCUSSION

**General Water Chemistry Characteristics.** For both detritus materials (pine and fir), the mass remaining decreased with increasing temperature, and was lower for thermal oxidation than pyrolysis (Figure 1A and Table S1). For both

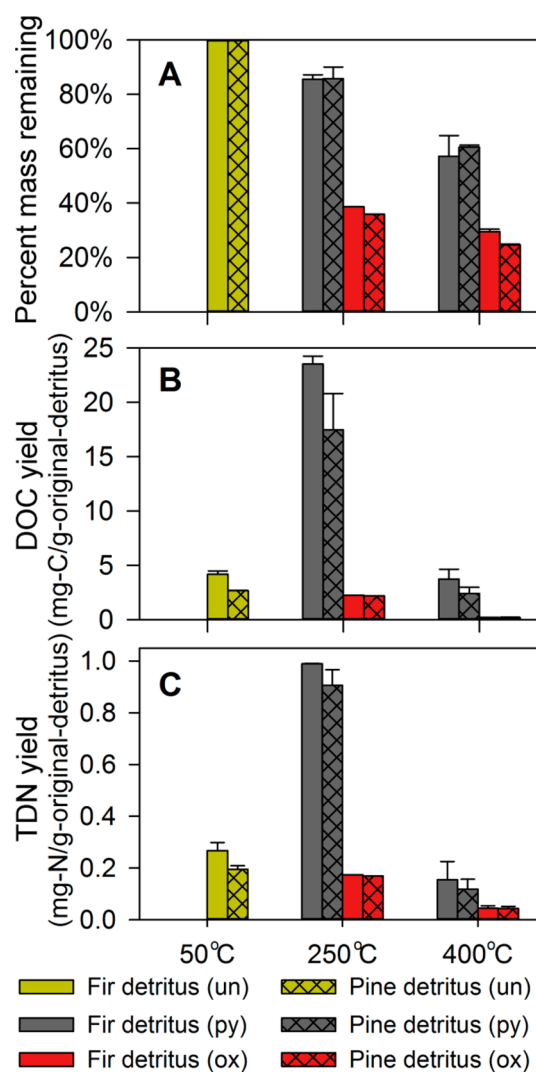


**Figure 1.** Percent mass remaining, dissolved organic carbon and total nitrogen yields from the controlled-lab-burned detritus material. Un, unburned; py, pyrolysis; ox, thermal oxidation.

pyrolysis and thermal oxidation, DOC and TDN levels decreased from 250 to 400 °C (Figure 1B,C). The 250py had much higher DOC (5.1 times) and TDN (4.2 times) than the unburned detritus. At the same burning temperature, the thermal oxidation consistently showed lower DOC and TDN levels compared to pyrolysis, consistent with the mass



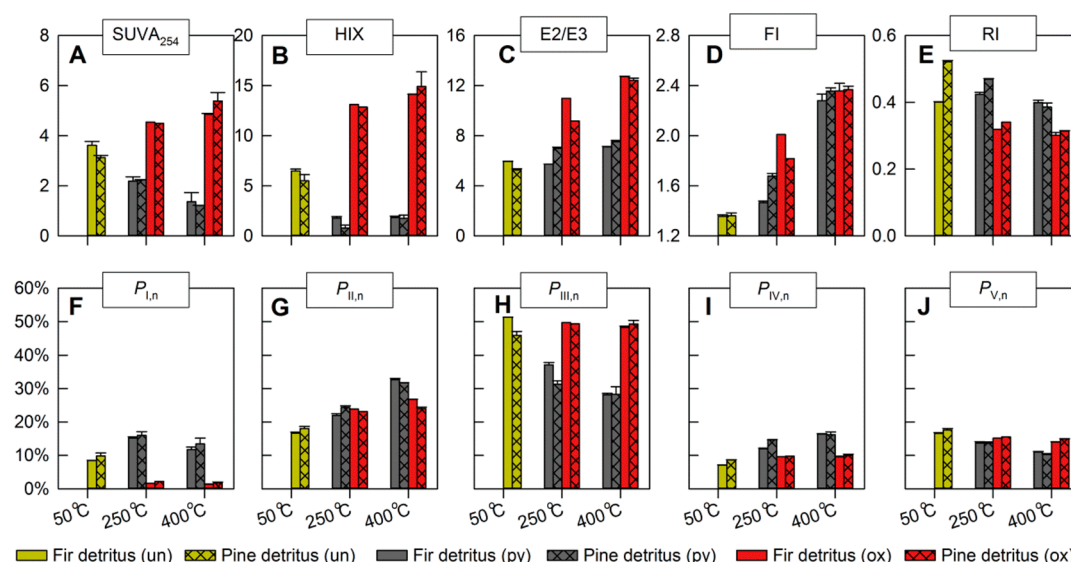


**Figure 2.** Optical properties of detritus extracts for controlled-lab-burned samples.  $SUVA_{254}$ , specific ultraviolet absorbance at 254 nm; E2/E3, UVA at 254 nm divided by UVA 365 nm; FI, fluorescence index; HIX, humification index; RI, redox index;  $P_{i,n}$ , the proportion of area-normalized volume in region  $i$  to the entire region based on fluorescence regional integration; Un, unburned; py, pyrolysis; ox, thermal oxidation.

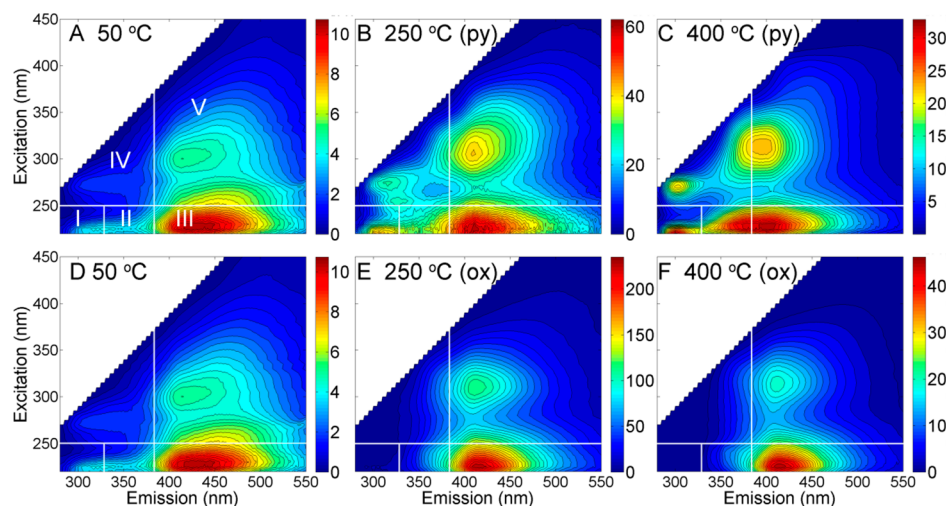


**Figure 3.** Fluorescence excitation–emission matrices of the water extracts from unburned and burned detritus taking ponderosa pine as an example. py: “pyrolysis”; ox: thermal oxidation.

remaining. More detailed water quality data for the water extracts are summarized in Table S1.

In contrast to field measurements at the Rim Fire, the DOM level was not always lower in burned ash than unburned detritus.<sup>16</sup> The lab-generated ash treatments suggest that when the burning temperature is low and pyrolysis dominates (e.g., 250 °C pyrolysis), the DOM level in the forest floor may be increased by fire. This observation is consistent with previous studies that show low-temperature pyrogenic chars (sometimes also called “brown carbon”) yield the highest DOM levels with a large proportion of *O*-alkyl components and limited aromatic structures.<sup>44</sup> The low-temperature degradation and depolymerization of cellulose via a transglycosylation pathway (peak yield at ~250–300 °C)<sup>44,45</sup> and lignocellulose components via cleavage of aryl–alkyl ether (C–O–C) linkages and dehydration (starting from 220 °C)<sup>46</sup> have been documented to significantly contribute to soluble organic matter during low temperature pyrogenic alterations.<sup>44</sup> Such temperature dependence for the DOM budget of forest detritus indicates that the

commonly severe forest wildfires and less-severe prescribed fires could result in distinctly different loads of terrestrial DOM and DBP precursors.

**Optical Characteristics.** Both temperature and oxygen availability significantly affected the UV–vis absorbance of the detritus extracts. Compared to that of unburned detritus extracts, the  $SUVA_{254}$  of burned detritus extracts increased after thermal oxidation and decreased after pyrolysis (Figure 2A). As the white ash from the previous field study<sup>16</sup> was likely formed from high-temperature oxidation,<sup>28</sup> our lab-burning results explain why the ash extracts from the field samples displayed mean  $SUVA_{254}$  values in the following order: white ash extracts > unburned detritus extracts > black ash extracts.<sup>16</sup> These results further explain why there were no consistently higher or lower  $SUVA_{254}$  values in fire-affected runoff or streamwater.<sup>17</sup> The consistently higher  $SUVA_{254}$  values in water extracts from thermally oxidized detritus suggest a higher aromaticity of the DOM compared to the pyrogenic ash. Such higher aromaticity in the thermally oxidized detritus was further confirmed by

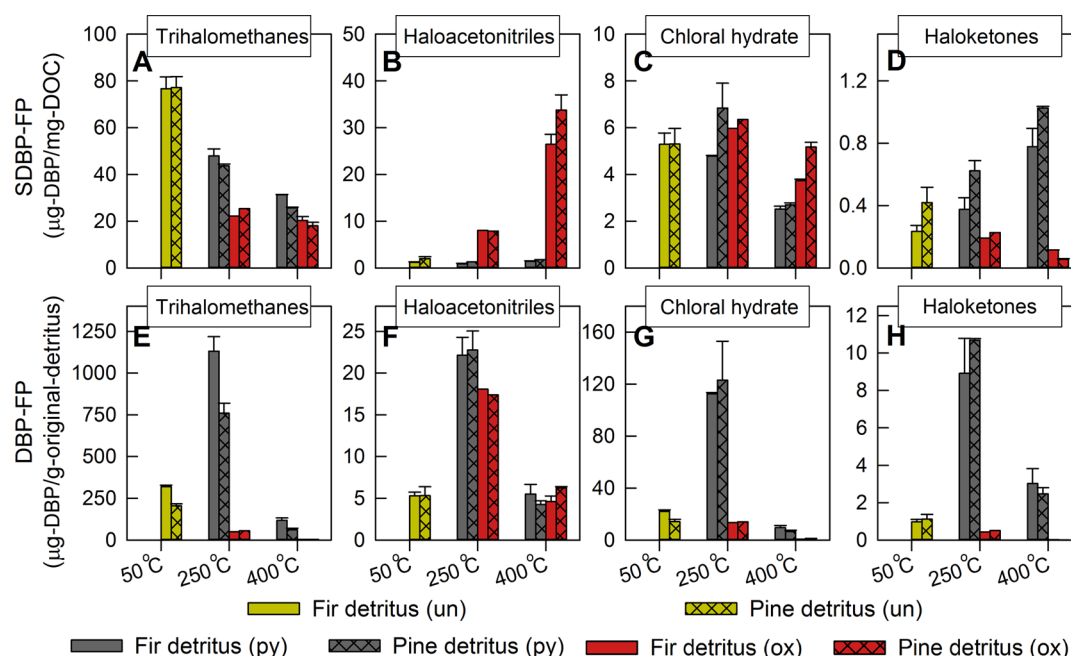


**Figure 4.** Reactivity of dissolved organic matter in forming disinfection byproducts (DBP) in detritus extracts as reflected by specific DBP formation potential (SDBP-FP) and the DBP formation potential of detritus (DBP-FP). Un, unburned; py, pyrolysis; ox, thermal oxidation.

molecular characterization of DOM using high-resolution FTICR-MS (Chow et al. in preparation).

Products of thermal oxidation usually have abundant hydrophilic oxygenated moieties (e.g., hydroxyl, carbonyl, and carboxyl groups), which endows the aromatic component in the combusted ash with a higher solubility. In contrast, the pyrogenic detritus can lose most of its hydrophilic groups and increase activated sites for sorption of aromatic DOM with increasing pyrolysis temperature,<sup>47</sup> thus causing a decrease in SUVA<sub>254</sub> in detritus extracts with increasing pyrolysis temperature. As E2/E3 negatively correlates with the molecular weight of DOM,<sup>33</sup> the higher E2/E3 in burned detritus compared to unburned detritus (Figure 3C) suggests that the fire-affected DOM has a lower molecular weight than nonburned DOM, particularly in oxidized ashes compared to pyrogenic ashes. This is consistent with FTICR-MS studies by Podgorski et al. that showed lower molecular weight of organic matter from thermally oxidized oak wood compared to unburned oak wood.<sup>26</sup>

The fluorescence EEM of the DOM showed a strong dependence on burning temperature and oxygen availability (Figure 3). Compared to the unburned-detritus extracts, the terrestrial-humic-like DOM peaks in EEM (A and C peaks<sup>36</sup>) were significantly reduced but the marine-humic-like DOM peak (M peak) increased in the burned-detritus extracts (Figure 3), while FI and  $\beta/\alpha$  were both increased for the burned detritus extracts (Figure 2D and Table S1). Whereas extracts of oxidized detritus showed consistently higher FI compared to the extracts of pyrogenic detritus at each temperature,  $\beta/\alpha$  was lower in extracts of 400ox detritus compared to 400py detritus. The higher FI and  $\beta/\alpha$  of DOM were also found in field ash samples from the Rim Fire compared to the unburned detritus.<sup>16</sup> This was attributed to fire-generated smaller and simpler DOM structures<sup>26</sup> that was fluorescent at the EEM location similar to the marine-humic-like DOM component.<sup>16,48</sup> Chemical fractionation of the fire-affected DOM in Vergnoux et al.<sup>48</sup> also indicates that the shift from terrestrial-

humic-like to marine-humic-like was mainly due to hydrophobic DOM rather than hydrophilic DOM.

This lab-burning study further confirmed that the fire-affected DOM had similar fluorescent properties to autochthonous DOM. However, the HIX in extracts of burned detritus, similar to the SUVA<sub>254</sub>, did not show consistently increased or decreased values compared to extracts of unburned detritus, but were highly dependent on oxygen availability (ox > unburned > py; Figure 2D). This result is also consistent with the field-observed ranking of mean HIX: white ash extract > unburned detritus extract > black ash extract.<sup>16</sup> The RI calculated from the Cory and McKnight PARAFAC model showed higher RI values (commonly more reduced) for extracts of unburned and pyrogenic detritus as compared to extracts of oxidized detritus (Figure 2E, Tables S1 and S2). This indicates that oxidized detritus had more chemically oxidized DOM than unburned and pyrogenic detritus. We also reanalyzed the EEMs of field samples from the Rim Fire and found similar results, i.e., significantly higher RI in black ash extracts (0.40–0.50;  $n = 15$ ) than white ash extracts (0.25–0.35;  $n = 15$ ).

The results of fluorescence regional integration (Figure 2F–J) indicate a high dependence of the fluorescent DOM composition on temperature and oxygen availability. At 250 and 400 °C, the percent fluorescence responses in region I (tyrosine-like) and region IV (microbial-byproduct-like) were significantly higher in extracts of pyrogenic detritus than oxidized detritus (Figure 2F,I). This may be caused by the release of amino-acid-like compounds from the pyrolytic depolymerization of detritus compared to the mineralization of the protein-like compounds during oxidation. The percent fluorescence response in region II of the EEM generally increased with increasing temperature and depended less on oxygen availability (Figure 2G), consistent with field observations of  $P_{\text{IIN}}$  for DOM: unburned detritus extracts < black ash extracts < white ash extracts.<sup>16</sup> The percent fluorescence response in regions III and V showed a significant decrease

from the unburned-detritus extracts to the pyrogenic-detritus extracts, but not from unburned-detritus extracts to the oxidized-detritus extracts (Figure 2H,J). This result clearly indicates that pyrolysis at higher temperatures promotes decomposition of fulvic/humic-like substances. This is consistent with the study of Lin et al.<sup>27</sup> who found humic substances decreased in hot-water extracts of pyrogenic sawdust biochar with higher pyrolysis temperature based on liquid chromatography and organic carbon detection and fluorescence analysis.

**DBP Precursors in Detritus Extracts.** As reflected by the SDBP-FP (Figure 4), the reactivity of DOM in forming DBPs was DBP-species-specific and highly dependent on the individual or interactive effects of temperature and oxygen availability (Table 1). There was no difference ( $P > 0.05$ )

**Table 1. Effects of Temperature (T), Oxygen Availability (O), Vegetation Type (V) and Their Interactions in Affecting Specific Disinfection Byproduct Formation Potential (SDBP-FP) of Detritus Extracts and the DBP Formation Potential (DBP-FP) of Burned Detritus Based on Three-Way ANOVA<sup>a</sup>**

	STHM-FP	SHAN-FP	SCHD-FP	SHK-FP	THM-FP	HAN-FP	CHD-FP	HK-FP
T	0.001	0.001	0.003	0.096	<0.001	<0.001	0.004	0.007
O	<0.001	<0.001	0.071	<0.001	<0.001	0.231	0.007	0.001
V	0.244	0.306	0.088	0.145	0.075	0.956	0.883	0.746
T*O	0.011	0.001	0.187	0.010	<0.001	0.146	0.012	0.013
T*V	0.363	0.333	0.700	0.749	0.165	0.948	0.811	0.548
O*V	0.171	0.393	0.839	0.115	0.069	0.806	0.908	0.768
T*O*V	0.578	0.330	0.193	0.752	0.151	0.529	0.817	0.573

<sup>a</sup>THMs, trihalomethanes; HANs, haloacetonitriles; CHD, chloral hydrate; HKs, halo ketones. Different colors indicate different level of significance: dark blue,  $P < 0.01$ ; medium blue,  $0.01 < P \leq 0.05$ ; light blue,  $0.05 < P \leq 0.1$ ; and no color,  $P > 0.1$ .

between vegetation type (pine vs fir) for SDBP-FP of burned detritus extracts (Table 1). Thus, this study focused on the effects of temperature and oxygen availability. After chlorination, THM was the most abundant DBP category, and the STHM-FP decreased with increasing temperature, from  $76.9 \pm 8.0 \mu\text{g-THMs/mg-DOC}$  for unburned detritus, to  $28.6 \pm 3.3 \mu\text{g-THMs/mg-DOC}$  for 400py detritus and  $19.3 \pm 2.9 \mu\text{g-THMs/mg-DOC}$  for 400ox detritus. The oxidized DOM had lower STHM-FP compared to pyrogenic DOM (Figure 4A). The SHAN-FP was similar for the unburned-detritus extracts ( $1.63 \pm 0.64 \mu\text{g-HANs/mg-DOC}$ ) and pyrogenic-detritus extracts, but increased from unburned-detritus extracts to the oxidized-detritus extracts (Figure 4B). The 400ox DOM had the highest reactivity in forming HANs ( $30.1 \pm 6.2 \mu\text{g-HANs/mg-DOC}$ ), which amounted to 18.7 times that of 400py DOM ( $1.61 \pm 0.25 \mu\text{g-HANs/mg-DOC}$ ). For chloral hydrate, the specific FP did not change significantly from unburned ( $5.30 \pm 0.95 \mu\text{g-CHD/mg-DOC}$ ) to 250 °C heating (pyrolysis,  $5.82 \pm 1.71 \mu\text{g-CHD/mg-DOC}$ ; oxidation,  $6.16 \pm 0.27 \mu\text{g-CHD/mg-DOC}$ ) but significantly decreased for the 400py DOM ( $4.45 \pm 0.87 \mu\text{g-CHD/mg-DOC}$ ; Figure 4C). For halo ketones, pyrolysis at 250 and 400 °C increased the specific FP to 1.5 and 2.8 times that of the unburned DOM ( $0.33 \pm 0.16 \mu\text{g-HKs/mg-DOC}$ ). In contrast, the 250 and 400 °C oxidation of detritus reduced the specific FP to 64 and 26% that of the unburned detritus, respectively (Figure 4D).

The SDBP-FP of DOM in this controlled-lab burning was highly consistent with the SDBP-FP dependence of DOM from the Rim Fire in terms of fire severity and DBP species.<sup>16</sup> In samples from the Rim Fire, the STHM-FP followed unburned detritus extract ( $46.6 \pm 12.5 \mu\text{g-THMs/mg-DOC}$ ) > black ash extract ( $28.4 \pm 4.6 \mu\text{g-THMs/mg-DOC}$ ) > white ash extract ( $22.7 \pm 8.3 \mu\text{g-THMs/mg-DOC}$ ); SHAN-FP followed unburned detritus extract ( $1.07 \pm 0.32 \mu\text{g-HANs/mg-DOC}$ ) < black ash extract ( $2.04 \pm 0.65 \mu\text{g-HANs/mg-DOC}$ ) < white ash extract ( $3.2 \pm 0.67 \mu\text{g-HANs/mg-DOC}$ ); and higher SHK-FP in black ash extract ( $0.54 \pm 0.12 \mu\text{g-HKs/mg-DOC}$ ) than unburned detritus extract ( $0.36 \pm 0.09 \mu\text{g-HKs/mg-DOC}$ ) and white ash extract ( $0.40 \pm 0.14 \mu\text{g-HKs/mg-DOC}$ ).

The decreased STHM-FP and increased SHAN-FP of DOM in burned detritus compared to unburned detritus strongly and directly supports that fire severity affected the chemistry of DOM and associated DBP formation as highlighted by the temperature and oxygen availability results of the lab study. Temperature and oxygen availability were both critical factors affecting the chlorine reactivity of DOM in forming DBPs ( $P \leq 0.01$ , except 0.096 for SHK-FP; Table 1). Comparing the burned and unburned detritus DOM, most changes in SDBP-FP were within the same order of magnitude, except for the SHAN-FP of 400ox DOM ( $30.1 \pm 6.2 \mu\text{g-HANs/mg-DOC}$ ), which was 18.7 times that of the unburned detritus DOM. Such high values of SHAN-FP are not common in most nitrogen-rich natural organic matter sources, such as bacterial/algal materials (commonly  $< 5 \mu\text{g-HANs/mg-DOC}$ ).<sup>42,43,49</sup> Some nitrogenous aromatics like aniline and indole (common fire-generated dissolved black nitrogen species<sup>50</sup>) are known to have very high reactivity in forming HANs;<sup>51</sup> however, it is still unclear what DOM chemical characteristics are the major contributor to HAN formation. Thus, HAN formation merits further investigation to clarify the molecular composition of HAN precursors in the thermally oxidized detritus.

Brominated DBPs have also been found to be more toxic than their chlorinated analogs.<sup>19</sup> Although the STHM-FP decreased after burning, the bromine incorporation factor of THMs significantly increased with increasing temperature, with consistently higher values for oxidized detritus than pyrogenic detritus at each temperature (Figure 5). Specifically, the bromine incorporation factor of THMs was 15–41% for 400ox DOM as compared to <1% for unburned DOM, 250 °C burned DOM, and 400 °C pyrogenic DOM. Similarly, the bromine incorporation factor of HANs was 2–4% for 400ox DOM as compared to <1% for others. Such result are consistent with the Rim Fire field study that showed higher bromide concentrations and brominated THMs from fire-affected DOM.<sup>16</sup> As bromide is well-known as a DBP precursor that facilitates brominated DBP formation,<sup>14</sup> the higher bromide concentrations especially in white ashes<sup>16</sup> are likely to be the major reason for the increased bromine incorporation factor. Importantly, the lab-burning results imply that low-severity fires may not cause increased formation of brominated DBPs, whereas severe burning with sufficient oxygen is more likely to contribute more bromide, which acts as a DBP precursor in source waters.

As determined by the quantity of DOM in detritus and its chlorine reactivity, the DBP-FPs for unburned detritus were  $261.9 \pm 67.9 \mu\text{g-THMs/g-original-detritus}$ ,  $5.29 \pm 1.33 \mu\text{g-HANs/g-original-detritus}$ ,  $18.04 \pm 5.19 \mu\text{g-CHD/g-original-detritus}$ , and  $1.04 \pm 0.34 \mu\text{g-HKs/g-original-detritus}$ . The DBP-FP of the burned detritus showed strong dependence on



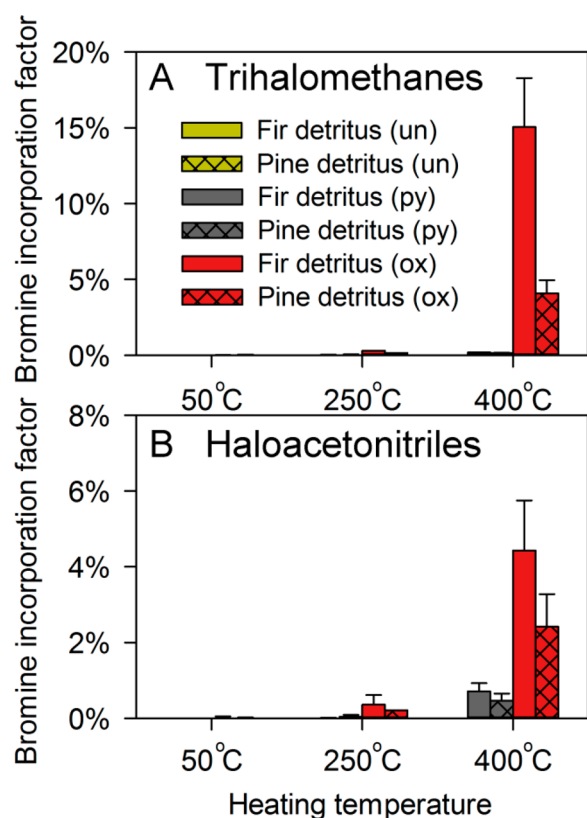


**Figure 5.** Bromine incorporation factor of trihalomethanes and haloacetonitriles formed from chlorination of dissolved organic matter from burned and unburned detritus extracts.

temperature, oxygen availability, and their interaction (Figure 4E–H and Table 1). In the Rim Fire field study, there was a consistent decrease in DBP-FP from the burned ash compared to unburned detritus.<sup>16</sup> However, the lab-burning study suggests that burning conditions, such as temperature and oxygen availability, can strongly affect the DBP-FP, which can result in significantly higher DBP-FP under some conditions. Particularly, the 250py had 5.1 times higher DOC than unburned detritus, and the DBP-FP was increased to  $945.7 \pm 246.0$   $\mu\text{g-THMs/g-original-detritus}$ ,  $22.4 \pm 3.64$   $\mu\text{g-HANs/g-original-detritus}$ ,  $117.8 \pm 35.2$   $\mu\text{g-CHD/g-original-detritus}$ , and  $9.80 \pm 2.40$   $\mu\text{g-HKs/g-original-detritus}$ . Therefore, the 250py had the highest formation potential for THMs (2.6 times higher than unburned detritus), HANs (3.2 times), CHD (5.5 times), and HKs (8.4 times). In contrast, the 250ox had relatively high HAN-FP ( $17.7 \pm 0.47$   $\mu\text{g-HANs/g-original-detritus}$ ; 3.3 times higher than unburned detritus); however, it had lower formation potentials for other DBPs (20.2% for THMs, 75.9% for CHD, and 44.8% for HKs compared to unburned detritus).

**Linking Chlorine Reactivity with Spectroscopic Characteristics.** Correlation analyses showed that the SDBP-FP for THMs, HANs, CHD, and HKs were significantly correlated with several spectroscopic characteristics (Table S3). A principal component analysis indicated two major principal components that explained 88.3% of the total variance (Table S4 and Figure S3); SHAN-FP, SHK-FP,  $\text{SUVA}_{254}$ , HIX, E2/E3,  $P_{\text{I,n}}$ ,  $P_{\text{III,n}}$ , and  $P_{\text{IV,n}}$  had a high loading on PC1; and STHM-FP, SCHD-FP, FI, RI,  $P_{\text{II,n}}$ , and  $P_{\text{V,n}}$  had a high loading on PC2. On the basis of the loading of different parameters, PC1 can be

considered as an axis mainly reflecting oxygen availability, and PC2 as an axis primarily reflecting heating temperature.

STHM-FP positively correlated with RI and  $P_{\text{V,n}}$  and negatively correlated with FI, E2/E3,  $P_{\text{II,n}}$ , and  $P_{\text{IV,n}}$  (Table S3), suggesting that the high-molecular-weight (low FI and low E2/E3) humic-like substances (high  $P_{\text{V,n}}$  and low  $P_{\text{II,n}}$  and  $P_{\text{IV,n}}$ ) from unaltered terrestrial sources (low FI and high RI) have the highest reactivity in forming THMs. This is consistent with the paradigm that terrestrial humic substances are highly reactive THM and HAA precursors.<sup>52</sup> Similarly, SCHD-FP had a relatively high loading on PC2, suggesting the unaltered terrestrial humic substances are also important CHD precursor. SHAN-FP was positively correlated with E2/E3, HIX,  $\text{SUVA}_{254}$ , and  $P_{\text{III,n}}$ , and negatively correlated with  $P_{\text{I,n}}$  and RI suggesting that the fire-altered low-molecular-weight (high E2/E3) oxidized (low RI) aromatic and humified (high  $\text{SUVA}_{254}$  and HIX) components have the highest reactivity in forming HANs. This is in agreement with our previous study<sup>16</sup> that showed the oxidized white ash had the highest SHAN-FP. As SHK-FP has a high negative loading on PC1 and had its highest values when the precursor was from the pyrogenic treatment having more reduced (high RI), less aromatic and humified (low  $\text{SUVA}_{254}$ , HIX,  $P_{\text{III,n}}$ , and  $P_{\text{V,n}}$ ) DOM.

**Implication for Wildfires and Water Quality.** Using field-burned detritus and unburned detritus to evaluate the effects of fire on DBP precursors provided us with important information to assess case-specific forest fire events.<sup>16</sup> However, as field-burned samples are always a composite containing ash derived from several contrasting fire elements (temperature, oxygen, fuel sources), the disadvantage of field studies is that the burned and unburned detritus cannot be perfectly matched making it difficult to interpret the individual effects of temperature and oxygen availability on ash characteristics.

Using controlled lab burning, this study clearly demonstrated that temperature and oxygen availability significantly affect the postburn DOM chemistry as reflected by optical properties and chlorine reactivity. Among all burned detritus, it was observed that with higher temperature and oxygen availability (i.e., higher fire severity),<sup>28</sup> there was a decrease in organic matter mass (as reflected by percent mass loss) and DOM (Figure 1). This implies that forest fire characteristics, such as smoldering combustion with low combustion efficiency versus flaming combustion with high efficiency, or crown and surface fires with more oxygen availability versus ground fires with lower oxygen availability, could have distinctly different consequences on the quantity of DOM in detritus and the associated DBP formation potential. Also, topography, wind conditions during the fire, soil depth (surface vs subsurface), and fuel size (large woody debris vs fine leaf litter) are critical factors determining the oxygen supply and burning efficiency. Thus, field studies incorporate a high degree of inherent spatial variation, often within short vertical or horizontal distances (a few centimeters), for example, white ash on the soil/wood surface and gray/black ash in a subsurface layer. Further, across different fire events, severe wildfires versus less-severe wildfires or prescribed fires could have highly different impacts on the DBP formation potential of detritus in forest floors. In particular, pyrolysis at 250 °C increased extractable DOC by 510% and the DBP formation potential per gram of original detritus by 261% THMs, 324% HANs, 553% CHD, and 840% HKs compared to unburned detritus. This suggests that low-temperature pyrogenic organic matter is an important contributor to the fire-affected DOM and DBP precursors in a watershed.

Wildfire behavior is highly contingent on the fuel properties (e.g., fuel load, chemistry, size, density, moisture content, heat content, compactness, etc.), weather (e.g., temperature, rainfall, humidity, wind, etc.), and topography (e.g., slope steepness, aspect, elevation, etc.). Several fire models<sup>53,54</sup> have been developed to understand and predict fire behavior and carbon dynamics but much information is still required before these fire-effects models can incorporate water quality impacts associated with contrasting fire conditions. The results of the current study provide important new information on incorporation of DOM into future models linking fire behavior and water quality. The results also provide important information for forest land managers to minimize DOM/DBP impacts related to fuel and fire management (e.g., forest thinning and prescribed fire) and for water resource managers to anticipate the potentially negative impacts of large fires on drinking water sources.

## ■ ASSOCIATED CONTENT

### ■ Supporting Information

The Supporting Information is available free of charge on the ACS Publications website at DOI: 10.1021/acs.est.5b03961.

Detailed data for water quality and fluorescence EEM; correlation and principal component analyses; the color of detritus under different treatments; sampling sites; and PCA loading. (PDF)

## ■ AUTHOR INFORMATION

### Corresponding Author

\*E-mail: [achow@clemson.edu](mailto:achow@clemson.edu). Tel.: +1 843 546 1013 x232. Fax: +1 843 546 6296.

### Notes

The authors declare no competing financial interest.

## ■ ACKNOWLEDGMENTS

This work was funded by NSF RAPID grant (1264579) and partially supported by NIFA/USDA (SC1700489 and 2014-67019-21615), and Joint Fire Science Program (14-1-06-19), as presented in technical contribution number 6396 of the Clemson University Experiment Station. J.W. thanks the China Scholarship Council (CSC[2011]3010) for financial support.

## ■ REFERENCES

- (1) Bladon, K. D.; Emelko, M. B.; Silins, U.; Stone, M. Wildfire and the future of water supply. *Environ. Sci. Technol.* **2014**, *48* (16), 8936–43.
- (2) Costanza, R.; d'Arge, R.; deGroot, R.; Farber, S.; Grasso, M.; Hannon, B.; Limburg, K.; Naeem, S.; O'Neill, R. V.; Paruelo, J.; Raskin, R. G.; Sutton, P.; vandenBelt, M. The value of the world's ecosystem services and natural capital. *Nature* **1997**, *387* (6630), 253–260.
- (3) Westerling, A. L.; Hidalgo, H. G.; Cayan, D. R.; Swetnam, T. W. Warming and earlier spring increase western US forest wildfire activity. *Science* **2006**, *313* (5789), 940–943.
- (4) van Mantgem, P. J.; Nesmith, J. C. B.; Keifer, M.; Knapp, E. E.; Flint, A.; Flint, L. Climatic stress increases forest fire severity across the western United States. *Ecol. Lett.* **2013**, *16* (9), 1151–1156.
- (5) Rhoades, C. C.; Entwistle, D.; Butler, D. The influence of wildfire extent and severity on streamwater chemistry, sediment and temperature following the Hayman Fire, Colorado. *Int. J. Wildland Fire* **2011**, *20* (3), 430–442.
- (6) Emelko, M. B.; Silins, U.; Bladon, K. D.; Stone, M. Implications of land disturbance on drinking water treatability in a changing climate: Demonstrating the need for "source water supply and protection" strategies. *Water Res.* **2011**, *45* (2), 461–472.
- (7) Silins, U.; Stone, M.; Emelko, M. B.; Bladon, K. D. Sediment production following severe wildfire and post-fire salvage logging in the Rocky Mountain headwaters of the Oldman River Basin, Alberta. *Catena* **2009**, *79* (3), 189–197.
- (8) Gonzalez-Perez, J. A.; Gonzalez-Vila, F. J.; Almendros, G.; Knicker, H. The effect of fire on soil organic matter - a review. *Environ. Int.* **2004**, *30* (6), 855–870.
- (9) Knicker, H. How does fire affect the nature and stability of soil organic nitrogen and carbon? A review. *Biogeochemistry* **2007**, *85* (1), 91–118.
- (10) Revchuk, A. D.; Suffet, I. H. Effect of wildfires on physicochemical changes of watershed dissolved organic matter. *Water Environ. Res.* **2014**, *86* (4), 372–381.
- (11) Mast, M. A.; Clow, D. W. Effects of 2003 wildfires on stream chemistry in Glacier National Park, Montana. *Hydrol. Processes* **2008**, *22* (26), 5013–5023.
- (12) Karanfil, T.; Krasner, S. W.; Westerhoff, P.; Xie, Y. F. *Disinfection by-products in drinking water: Occurrence, formation, health effects, and control*. Oxford University Press, USA, 2008; ACS Symposium Series 995.
- (13) Xie, Y. F. *Disinfection Byproducts in Drinking Water: Formation, Analysis, and Control*. CRC Press: Boca Raton, Florida, USA, 2004.
- (14) Chow, A. T.; Dahlgren, R. A.; Harrison, J. A. Watershed sources of disinfection byproduct precursors in the Sacramento and San Joaquin rivers, California. *Environ. Sci. Technol.* **2007**, *41* (22), 7645–7652.
- (15) Mikkelsen, K. M.; Dickenson, E. R. V.; Maxwell, R. M.; McCray, J. E.; Sharp, J. O. Water-quality impacts from climate-induced forest die-off. *Nat. Clim. Change* **2013**, *3* (3), 218–222.
- (16) Wang, J. J.; Dahlgren, R. A.; Ersan, M. S.; Karanfil, T.; Chow, A. T. Wildfire altering terrestrial precursors of disinfection byproducts in forest detritus. *Environ. Sci. Technol.* **2015**, *49* (10), 5921–5929.
- (17) Writer, J. H.; Hohner, A.; Oropeza, J.; Schmidt, A.; Cawley, K. M.; Rosario-Ortiz, F. L. Water treatment implications after the High Park Wildfire, Colorado. *J. Am. Water Works Ass.* **2014**, *106* (4), E189–E199.
- (18) Majidzadeh, H.; Wang, J. J.; Chow, A. T. Prescribed fire altered dissolved organic matter and disinfection by-product precursors in forested watersheds - Part I. A controlled laboratory study. In *Recent Advances in Disinfection By-Products*, Karanfil, T., Ed. American Chemical Society: 2015; p 271–292.
- (19) Richardson, S. D.; Plewa, M. J.; Wagner, E. D.; Schoeny, R.; DeMarini, D. M. Occurrence, genotoxicity, and carcinogenicity of regulated and emerging disinfection by-products in drinking water: A review and roadmap for research. *Mutat. Res., Rev. Mutat. Res.* **2007**, *636* (1–3), 178–242.
- (20) Brewer, C. E.; Schmidt-Rohr, K.; Satrio, J. A.; Brown, R. C. Characterization of biochar from fast pyrolysis and gasification systems. *Environ. Prog. Sustainable Energy* **2009**, *28* (3), 386–396.
- (21) Soucemarianadin, L. N.; Quideau, S. A.; MacKenzie, M. D.; Bernard, G. M.; Wasylishen, R. E. Laboratory charring conditions affect black carbon properties: A case study from Quebec black spruce forests. *Org. Geochem.* **2013**, *62*, 46–55.
- (22) Kluepfel, L.; Keiluweit, M.; Kleber, M.; Sander, M. Redox properties of plant biomass-derived black carbon (biochar). *Environ. Sci. Technol.* **2014**, *48* (10), S601–S611.
- (23) Keiluweit, M.; Nico, P. S.; Johnson, M. G.; Kleber, M. Dynamic molecular structure of plant biomass-derived black carbon (biochar). *Environ. Sci. Technol.* **2010**, *44* (4), 1247–1253.
- (24) Uchimiya, M.; Ohno, T.; He, Z. Q. Pyrolysis temperature-dependent release of dissolved organic carbon from plant, manure, and biorefinery wastes. *J. Anal. Appl. Pyrolysis* **2013**, *104*, 84–94.
- (25) Jamieson, T.; Sager, E.; Gueguen, C. Characterization of biochar-derived dissolved organic matter using UV-visible absorption



and excitation-emission fluorescence spectroscopies. *Chemosphere* **2014**, *103*, 197–204.

(26) Podgorski, D. C.; Hamdan, R.; McKenna, A. M.; Nyadong, L.; Rodgers, R. P.; Marshall, A. G.; Cooper, W. T. Characterization of pyrogenic black carbon by desorption atmospheric pressure photo-ionization Fourier transform ion cyclotron resonance mass spectrometry. *Anal. Chem.* **2012**, *84* (3), 1281–1287.

(27) Lin, Y.; Munroe, P.; Joseph, S.; Henderson, R.; Ziolkowski, A. Water extractable organic carbon in untreated and chemical treated biochars. *Chemosphere* **2012**, *87* (2), 151–157.

(28) Bodi, M. B.; Martin, D. A.; Balfour, V. N.; Santin, C.; Doerr, S. H.; Pereira, P.; Cerda, A.; Mataix-Solera, J. Wildland fire ash: Production, composition and eco-hydro-geomorphic effects. *Earth-Sci. Rev.* **2014**, *130*, 103–127.

(29) Bird, M. I.; Wynn, J. G.; Saiz, G.; Wurster, C. M.; McBeath, A. The pyrogenic carbon cycle. *Annu. Rev. Earth Planet. Sci.* **2015**, *43*, 273–298.

(30) Chow, A. T.; Dai, J. N.; Conner, W. H.; Hitchcock, D. R.; Wang, J. J. Dissolved organic matter and nutrient dynamics of a coastal freshwater forested wetland in Winyah Bay, South Carolina. *Biogeochemistry* **2013**, *112* (1–3), 571–587.

(31) Zhou, J.; Wang, J. J.; Baudon, A.; Chow, A. T. Improved fluorescence excitation-emission matrix regional integration to quantify spectra for fluorescent dissolved organic matter. *J. Environ. Qual.* **2013**, *42* (3), 925–930.

(32) Karanfil, T.; Schlautman, M. A.; Erdogan, I. Survey of DOC and UV measurement practices with implications for SUVA determination. *J. Am. Water Works Ass.* **2002**, *94* (12), 68–80.

(33) Peuravuori, J.; Pihlaja, K. Molecular size distribution and spectroscopic properties of aquatic humic substances. *Anal. Chim. Acta* **1997**, *337* (2), 133–149.

(34) Murphy, K. R.; Butler, K. D.; Spencer, R. G. M.; Stedmon, C. A.; Boehme, J. R.; Aiken, G. R. Measurement of dissolved organic matter fluorescence in aquatic environments: An interlaboratory comparison. *Environ. Sci. Technol.* **2010**, *44* (24), 9405–9412.

(35) Chen, W.; Westerhoff, P.; Leenheer, J. A.; Booksh, K. Fluorescence excitation - emission matrix regional integration to quantify spectra for dissolved organic matter. *Environ. Sci. Technol.* **2003**, *37* (24), 5701–5710.

(36) Fellman, J. B.; Hood, E.; Spencer, R. G. M. Fluorescence spectroscopy opens new windows into dissolved organic matter dynamics in freshwater ecosystems: A review. *Limnol. Oceanogr.* **2010**, *55* (6), 2452–2462.

(37) Cory, R. M.; McKnight, D. M. Fluorescence spectroscopy reveals ubiquitous presence of oxidized and reduced quinones in dissolved organic matter. *Environ. Sci. Technol.* **2005**, *39* (21), 8142–8149.

(38) Wilson, H. F.; Xenopoulos, M. A. Effects of agricultural land use on the composition of fluvial dissolved organic matter. *Nat. Geosci.* **2009**, *2* (1), 37–41.

(39) Ohno, T. Fluorescence inner-filtering correction for determining the humification index of dissolved organic matter. *Environ. Sci. Technol.* **2002**, *36* (4), 742–746.

(40) Krasner, S.; Scimanti, M. In *Characterization of natural organic matter: Disinfection by-product analysis*, Natural Organic Matter In Drinking Water: Origin, Characterization, and Removal: Workshop Proceedings, 1993; p 9.

(41) Summers, R. S.; Hooper, S. M.; Shukairy, H. M.; Solarik, G.; Owen, D. Assessing the DBP yield: Uniform formation conditions. *J. Am. Water Works Ass.* **1996**, *88* (6), 80–93.

(42) Wang, J. J.; Ng, T. W.; Zhang, Q.; Yang, X. B.; Dahlgren, R. A.; Chow, A. T.; Wong, P. K. Reactivity of C1 and C2 organohalogen formation – from plant litter to bacteria. *Biogeochemistry* **2012**, *9* (10), 3721–3727.

(43) Wang, J. J.; Liu, X.; Ng, T. W.; Xiao, J. W.; Chow, A. T.; Wong, P. K. Disinfection byproduct formation from chlorination of pure bacterial cells and pipeline biofilms. *Water Res.* **2013**, *47* (8), 2701–2709.

(44) Norwood, M. J.; Louchouart, P.; Kuo, L. J.; Harvey, O. R. Characterization and biodegradation of water-soluble biomarkers and organic carbon extracted from low temperature chars. *Org. Geochem.* **2013**, *56*, 111–119.

(45) Harvey, O. R.; Herbert, B. E.; Kuo, L. J.; Louchouart, P. Generalized two-dimensional perturbation correlation infrared spectroscopy reveals mechanisms for the development of surface charge and recalcitrance in plant-derived biochars. *Environ. Sci. Technol.* **2012**, *46*, 10641–10650.

(46) Haw, J. F.; Schultz, T. P. <sup>13</sup>C CP/MAS NMR and FT-IR study of low-temperature lignin pyrolysis. *Holzforschung* **1985**, *39*, 289–296.

(47) Chen, B. L.; Zhou, D. D.; Zhu, L. Z. Transitional adsorption and partition of nonpolar and polar aromatic contaminants by biochars of pine needles with different pyrolytic temperatures. *Environ. Sci. Technol.* **2008**, *42* (14), 5137–5143.

(48) Vergnoux, A.; Di Rocco, R.; Domeizel, M.; Guiliano, M.; Doumenq, P.; Theriault, F. Effects of forest fires on water extractable organic matter and humic substances from Mediterranean soils: UV-vis and fluorescence spectroscopy approaches. *Geoderma* **2011**, *160*, 434–443.

(49) Fang, J. Y.; Ma, J.; Yang, X.; Shang, C. Formation of carbonaceous and nitrogenous disinfection by-products from the chlorination of *Microcystis aeruginosa*. *Water Res.* **2010**, *44* (6), 1934–1940.

(50) Knicker, H. How does fire affect the nature and stability of soil organic nitrogen and carbon? A review. *Biogeochemistry* **2007**, *85* (1), 91–118.

(51) Bull, R. J.; Reckhow, D. A.; Rotello, V.; Bull, O. M.; Kim, J. *Use of Toxicological and Chemical Models to Prioritize DBP Research*. American Water Works Association Research Foundation, Denver, CO, USA, 2006.

(52) Singer, P. C. Humic substances as precursors for potentially harmful disinfection by-products. *Water Sci. Technol.* **1999**, *40*, 25–30.

(53) Smithwick, E. A. H.; Ryan, M. G.; Kashian, D. M.; Romme, W. H.; Tinker, D. B.; Turner, M. G. Modeling the effects of fire and climate change on carbon and nitrogen storage in lodgepole pine (*Pinus contorta*) stands. *Global Change Biol.* **2009**, *15* (3), 535–548.

(54) Kashian, D. M.; Romme, W. H.; Tinker, D. B.; Turner, M. G.; Ryan, M. G. Carbon storage on landscapes with stand-replacing fires. *BioScience* **2006**, *56* (7), 598–606.